

R. V. Kirkham

802851

*Rec'd
8/10/89*

GEOCHEMISTRY AND HYDROTHERMAL ALTERATION ZONING
OF THE WHITING CREEK STOCKWORK MOLYBDENUM DEPOSIT
TAHTSA LAKE AREA, BRITISH COLUMBIA

*Graded Thesis
RS 24*

by

Morrie David Goodz

A thesis submitted to the Faculty of
Science in partial fulfillment of
the requirements for the degree of
Bachelor of Science
(Honours)

Department of Geology
Carleton University
Ottawa, Ontario
March, 1982

The undersigned hereby recommend to the Faculty of Science acceptance of this thesis, submitted by Morrie David Goodz, in partial fulfillment of the requirements for the degree of Bachelor of Science with Honours.

.....
Thesis Supervisor

.....
Chairman, Department of Geology



Figure 1: View of the southern slopes of Sibola Peak (7101 feet). The Whiting Creek deposit is located on the treed right-centre limb of the mountain.

ABSTRACT

Whiting Creek in the Tahtsa Lake area of west central British Columbia is composed of two alkali-calcic series granite "quartz porphyry" plugs bisected by monzonitic intrusive rocks. The quartz porphyry contains molybdenite in veinlets and quartz stockworks with or without pyrite.

Hydrothermal alteration in the quartz porphyry is exhibited by the quartz-sericite-pyrite (phyllic) assemblage. Sericite and K-feldspar have formed at the expense of plagioclase. There are no ferromagnesium minerals present.

Element concentration by thermogravitational diffusion has resulted in enrichment of SiO_2 , K_2O , Al_2O_3 , F, Rb, and Mo, and depletion of TiO_2 , total Fe, MgO and MnO. Depletion of Na_2O and CaO is due to hydrothermal alteration.

Petrographic, mineralization, alteration, and chemical features at Whiting Creek, are typical of a stock-work molybdenum deposit of the Climax transitional-type.

TABLE OF CONTENTS

Abstract	iv
Table of Contents	v
List of Figures	vii
List of Tables	viii
CHAPTER 1 - INTRODUCTION	2
1.1 Location and History	2
1.2 Purpose and Methods	3
1.3 Acknowledgements	4
CHAPTER 2 - REGIONAL GEOLOGY	5
2.1 General Geology	5
2.2 Structural Geology	8
2.3 Mineral Occurrences related to the Bulkley Intrusions	8
2.4 Evolution of the Plutonic Centre	9
CHAPTER 3 - THE WHITING CREEK DEPOSIT	11
3.1 Morphology and Structure	11
3.2 Petrography of the Deposit	11
3.2.1 Host Rocks	11
3.2.2 Facies and Extent of Hydrothermal Alteration	20
3.2.3 Sulphide Mineralogy	22
CHAPTER 4 - CHEMISTRY OF THE DEPOSIT	25
4.1 Chemical Zonation with the Quartz Porphyry	26
4.2 Effect and Similarity between Alteration, Mineralization and Chemistry	31
4.3 Summary	

CHAPTER 5 - GENESIS AND CLASSIFICATION OF STOCKWORK MOLYBDENUM DEPOSITS	36
5.1 General Description	36
5.2 Whiting Creek	38
CHAPTER 6 - CONCLUSIONS	42
References	45
Appendix I	47
Appendix II	48
Appendix III	49
Appendix IV	50
Appendix V	51

LIST OF FIGURES

Figure 1:	View of the southern slopes of Sibola Peak (7101 feet)	iii
Figure 2:	Location map of the Whiting Creek deposit	1
Figure 3:	General geology of the Sibola Peak area	6
Figure 4:	Detailed geology of the Whiting Creek deposit	12
Figure 5:	Sample and drill hole location map	13
Figure 6a:	Outcrop of quartz porphyry (sample site #1); note quartz stockwork with and without molybdenite	15
6b:	Quartz porphyry showing unaltered quartz and sericitized feldspar phenocrysts; molybdenite veins with ferri-molybdenite and limonite coatings	15
Figure 7a:	Corroded quartz phenocryst surrounded by a quartz-potassium feldspar-sericite groundmass	17
7b:	Magnification of the corroded interface	17
Figure 8:	Fine grained, prismatic molybdenite crystals in a quartz vein	19
Figure 9:	Qualitative degree of phyllic alteration across the quartz porphyry (QPP)	21
Figure 10:	Metalliferous zones	23
Figure 11:	Variation of SiO_2 (weight per cent) across the QPP	27
Figure 12:	Ternary plot of normative quartz-albite-orthoclase ratios of the QPP	28
Figure 13:	Variation of K_2O (weight per cent) across the QPP	29
Figure 14:	Variation of normative corundum across the QPP	30
Figure 15:	Variation of fluorine (parts per million) across the QPP	32

LIST OF TABLES

Table 1:	Table of formations	7
Table 2:	Whole rock analyses of Bulkley intrusions	34
Table 3:	General characteristics of stockwork molybdenum deposits	39
Table 4:	Chemical analyses of altered granite rocks	41

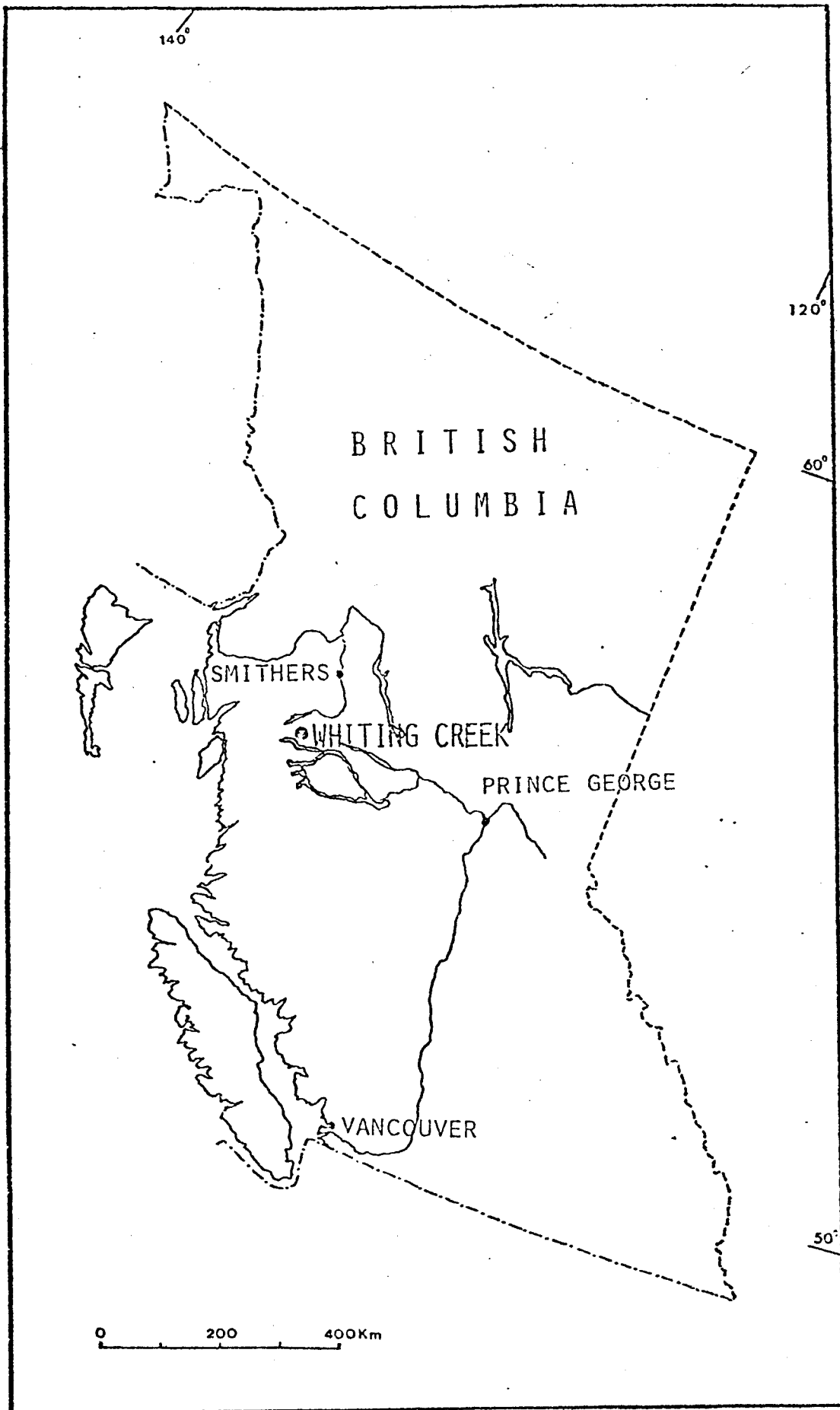


Figure 2: Location map of the Whiting Creek deposit

CHAPTER I - INTRODUCTION

The Whiting Creek deposit is a large low grade molybdenum prospect in the Intermontane Belt of the Canadian Cordillera, that resembles the "Climax-type 'transitional'" stockwork molybdenum deposits of Westra and Keith (1981).

Molybdenite is associated with two small quartz porphyry stocks of late Cretaceous age that intrude Jurassic volcanic rocks. Hypogene mineralization is restricted to (1) fracture controlled and disseminated pyrite, and (2) quartz stockworks with molybdenite and, locally, pyrite. Chalcopyrite and bornite are rare.

1.1 Location and History

The Whiting Creek deposit is in the Omineca Mining Division, west-central British Columbia (NTS 93E/11,14) at latitude 53°45'N and longitude 127°13'W (Figure 2). It is situated 12 km north of Tahtsa Lake and 90 km southwest of Houston from where it can be reached by forestry gravel access roads.

Prospecting in the Sibola Ranges began in the early 1900's with the discovery of vein-type deposits. In 1913, the discovery of placer gold and its source on Sibola Peak was followed by a rush of claim staking. Lead-zinc-silver and copper deposits were subsequently located, most

notable of which was the Emerald Glacier deposit on Mount Sweeney.

With construction of the François-Tahtsa Lake access road by Alcan in 1947, the area became readily accessible, and interest in mineral deposits was renewed. This interest peaked in the late 1960's with exploration focussed mainly toward large tonnage deposits amenable to open-pit mining. Kennco Explorations Western Ltd., in particular, conducted extensive geochemical and geophysical exploration programmes, and found a large number of copper-molybdenum and molybdenum occurrences, including Whiting Creek.

The property first explored in 1964 consisted of fifty claims (WHIT) located on the south slope of Sibola Peak, at elevations of 1150 - 1800 metres (Figure 1). From 1964 to 1965, 3245 feet of diamond drilling in twenty-one holes and over 24,000 lineal feet of trenching were conducted. In 1972, Quintana Mines Ltd. drilled one hole to a depth of 1400 feet.

SMD Mining Co. Ltd. gained control of the property in 1979 and have since drilled nineteen diamond holes, which have outlined a large low grade molybdenum deposit.

1.2 Purpose and Methods

The purpose of this study was to document the geology, chemistry, and hydrothermal alteration of the Whiting Creek "porphyry-type" molybdenum deposit.

During the 1981 field season, the writer mapped an area 1.5 X 0.5 km at a scale of 1:5000. Thirty-seven surface samples and twenty-six diamond drill hole core samples from four holes were collected. Sixty-six thin sections and eleven polished thin sections were examined, and both major and minor elemental analysis were performed on thirty-three samples.

1.3 Acknowledgements

The author gratefully acknowledges SMD Mining Co. Ltd. for financial and research support. Also the supervisory field assistance by Bob Cann and Dave Chan was appreciated.

I am indebted to Dr. Ian Jonasson, my supervisor, for his guidance and funding of chemical analyses and thin section preparation. Special thanks are extended to Dr. Dave Watkinson for the many constructive criticisms he suggested throughout this study. Stimulating and critical discussions with Dr. Dave Sinclair and computer processing of chemical data by Dr. Jim Franklin helped to shape the final interpretation of ore genesis model.

Finally, I would like to thank Debbie Forrest for drafting services and Julie Hunt for typing the manuscript.

CHAPTER 2 - REGIONAL GEOLOGY

2.1 General Geology

Previous geological mapping of the region was conducted by M.S. Hedley (1935) and S. Duffell (1959) of the Geological Survey of Canada. Recent studies with emphasis on the Tahtsa Lake district were made by N.C. Carter (1974) and D.G. MacIntyre (1976-78).

Geology of the Sibola Peak area is shown in Figure 3. The major geological formations in the area are summarized in Table 1. The most significant of these, in terms of areal extent, is the Hazelton group, a 3 km thickness of interbedded volcanic and sedimentary rocks of early to middle Jurassic age (Duffell, 1959). These rocks have been deformed in broad open folds and regionally metamorphosed to greenschist facies.

Rocks of the Hazelton group are intruded by a series of late Cretaceous granodiorite to quartz monzonite stocks and dyke swarms that range in age from 70 to 84 m.y. (Carter, 1974). These plutonic rocks are known as the Bulkley intrusions. These oval and elongate stocks usually range from 0.5 to 4 km in diameter. They have been localized in part, by north to northwest-trending faults. Associated with these plutons and related dykes are copper-molybdenum and molybdenum deposits.

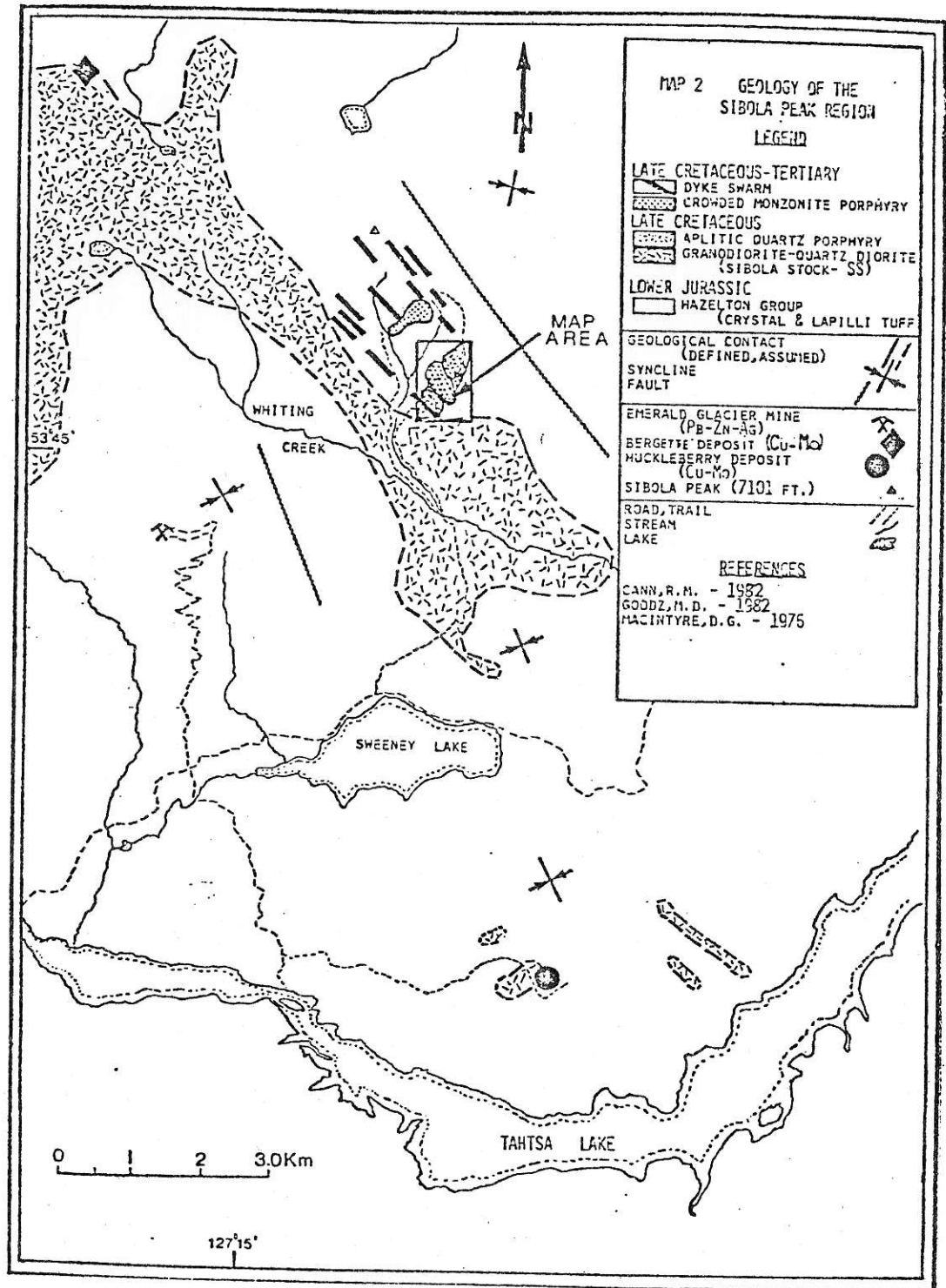


Figure 3: General geology of the Sibola Peak area

TABLE 1 - TABLE OF FORMATIONS

Phanerozoic

CENOZOIC

Quarternary

Recent and
PleistoceneGlacial
debris:

till, gravel, sand

Unconformity

MESOZOIC

Late Cretaceous

Bulkley
intrusions:
(70-84m.y.)hornblende feldspar
porphyry, monzonite
porphyry, quartz
monzonite, quartz
porphyry, granodio-
rite-quartz diorite

Angular Unconformity

Lower to Middle
JurassicHazelton
groupandesitic pyroclas-
tic rocks

2.2 Structural Geology

The Sibola Peak district is along the western periphery of the Intermontane Thrust and Fold belt, which consists of folded eugeosynclinal rocks, known as the Nechako Trough.

The area has been subjected to a complex history of faulting and regional uplift related to the evolution of the Pacific Orogen. The major structural elements in the area are high angle normal and reverse faults, which bound uplifted, down-faulted, and tilted blocks (MacIntyre, 1976).

The prominent trend of faulting is northwest, with subordinate northeast and north-trending faults.

MacIntyre and Hodder (1978) interpreted a fault-bounded circular area centred on Tahtsa Lake as a collapsed caldera. They concluded that the Bulkley intrusions and attendant mineralization are temporally associated with post-collapse resurgence of magma.

2.3 Mineral Occurrences Related to the Bulkley Intrusions

The Bulkley intrusions have been subdivided into three phases of emplacement at 70 m.y., 76 m.y., and 83 m.y. (Carter, 1974). Spatially associated with these are occurrences of chalcopyrite and molybdenite, mainly as disseminations or in stockwork quartz veinlets, with coincident gangue mineral assemblages attributed to hydrothermal alteration. Mineralogical, morphological, and textural criteria, match those of "porphyry-type" deposits.

Multiple intrusions are a feature of several occurrences, along with late post-mineralization dykes. Mesozoic volcanic and sedimentary rocks adjacent to the intrusions have been metamorphosed to biotite hornfels. Weathering of associated pyritic haloes often results in the formation of prominent gossans which can be used as exploration guides. Supergene enrichment is minimal, if present at all.

2.4 Evolution of the Plutonic Centre

A sequence of events in the formation of the stratigraphic column of Sibola Peak is as follows:

- (1) Andesitic volcanic rocks along with clastic and chemical sedimentary rocks were deposited as part of a volcanic island arc-trench complex built on the continental margin during lower to middle Jurassic time. These rocks comprise the Hazelton group.
- (2) To the south of the map region, Hazelton group rocks were unconformably overlain by sedimentary and volcanic rocks of the Skeena group. Subsequent erosion and then deposition of a sedimentary sequence known as the Kasalka group was followed by the Kasalka felsic intrusions. Abrupt subsidence along arcuate and radial faults, centred on Tahtsa Lake, resulted in a collapsed caldera.

- (3) Tension fractures related to the caldera acted as conduits for magma resurgence, resulting in the emplacement of granodiorite stocks at 82 to 83 m.y. These stocks were the first of the Bulkley series of intrusions. Extensive copper-molybdenum mineralization associated with these stocks also occurred at this time. The region had now become part of a continental volcanic arc regime.
- (4) A second magmatic resurgence at 74 to 76 m.y. resulted in the emplacement of the compositionally-zoned granodiorite to quartz diorite Sibola stock. Dyke swarms of quartz monzonite to granite composition occupied post-resurgence tension fractures along northwest-trending rifts. Smaller and lower grade copper and molybdenum bodies such as at Whiting Creek are associated with this second subdivision of the Bulkley intrusions.
- (5) Deep erosion of the volcanic cover and unroofing of the plutonic rocks preceded formation of the Coast Plutonic range.

CHAPTER 3 - THE WHITING CREEK DEPOSIT

3.1 Morphology and Structure

Detailed geology of Whiting Creek and sample locations are given in Figures 4 and 5. The deposit is localized in a quartz porphyry intrusion. Molybdenite occurs mainly in fractures and quartz stockworks, and to a lesser extent, as disseminated grains.

The quartz porphyry (QPP) is exposed in two plugs, centred at elevations of 1450 and 1600 metres, on a southern limb of Sibola Peak. Northwest-trending dyke swarms crosscut and possibly bisect what may have been originally a single QPP pluton. Chemical trends and alteration zoning support the hypothesis of pluton bisection.

3.2 Petrography of the Deposit

3.2.1 Host Rocks

Early to Middle Jurassic

Hazelton Group

In the map area, the Hazelton group comprises principally an andesitic pyroclastic assemblage of green crystal, lapilli, and lithic tuffs. The volcanic rocks have been regionally metamorphosed to greenschist facies, with contact metamorphism to biotite hornfels, present immediately adjacent to an intrusion.

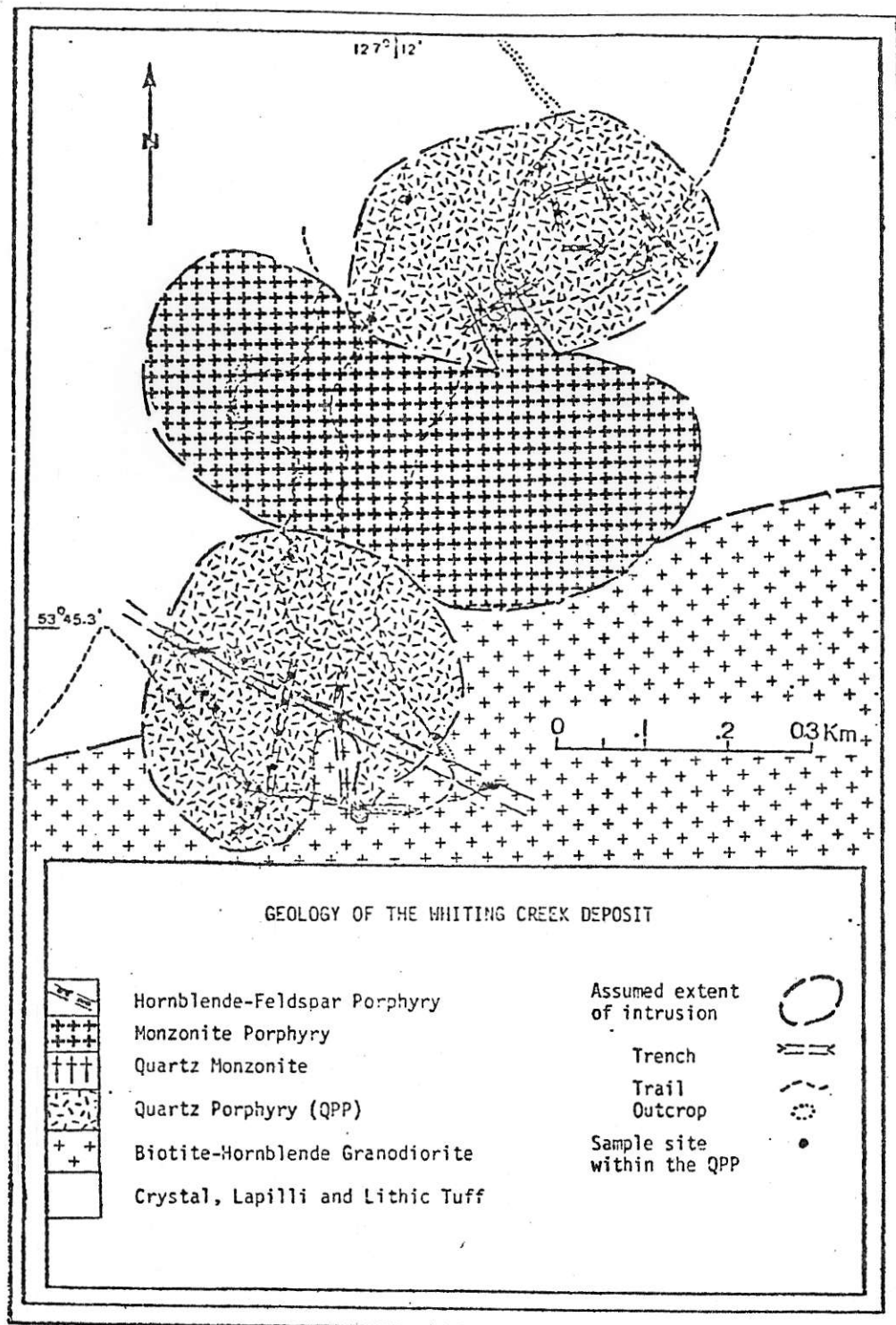


Figure 4: Detailed geology of the Whiting Creek deposit

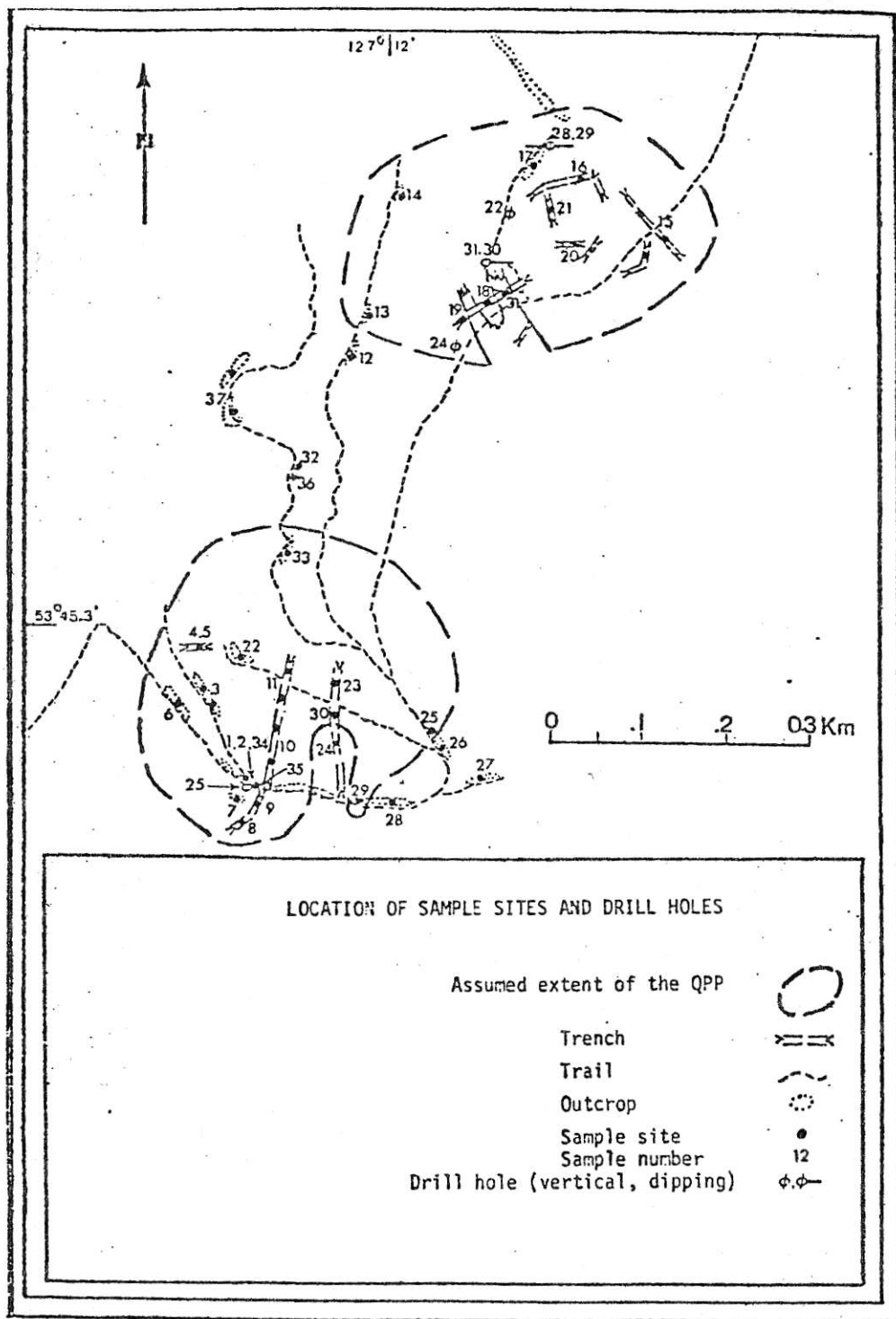


Figure 5: Sample and drill hole location map

Upper Cretaceous

Bulkley Intrusions

The Bulkley intrusions as defined by Carter (1974) for the Whiting Creek area, are (1) those compositional-zoned granodiorite to quartz diorite intrusions, and magmatic differentiates of the second subdivision (74 - 76 m.y.). The magmatic differentiates are (2) plugs of granite composition within and peripheral to (1), and (3) late, northwest-trending porphyritic monzonite dyke swarms cutting both (1) and (2).

Biotite-Hornblende Granodiorite:

A large, compositionally-zoned stock of bulk granodiorite to quartz diorite composition, known as the Sibola stock, intrudes Hazelton group rocks. In the map area it is represented by biotite-hornblende granodiorite (GRDR).

The rocks exhibit a hypidiomorphic granular texture consisting of closely packed euhedral, oscillatory-zoned, oligoclase-andesine laths, 1 to 5 mm in length. Interstitial are fine to medium grained (0.5 to 3 mm) quartz, K-feldspar, and hornblende crystals. There has been weak kaolinization of the plagioclase and biotitization and chloritization of fifty per cent of the hornblende.

Quartz Porphyry

Two small irregular plugs of granite composition are within and peripheral to the GRDR stock. These plugs of

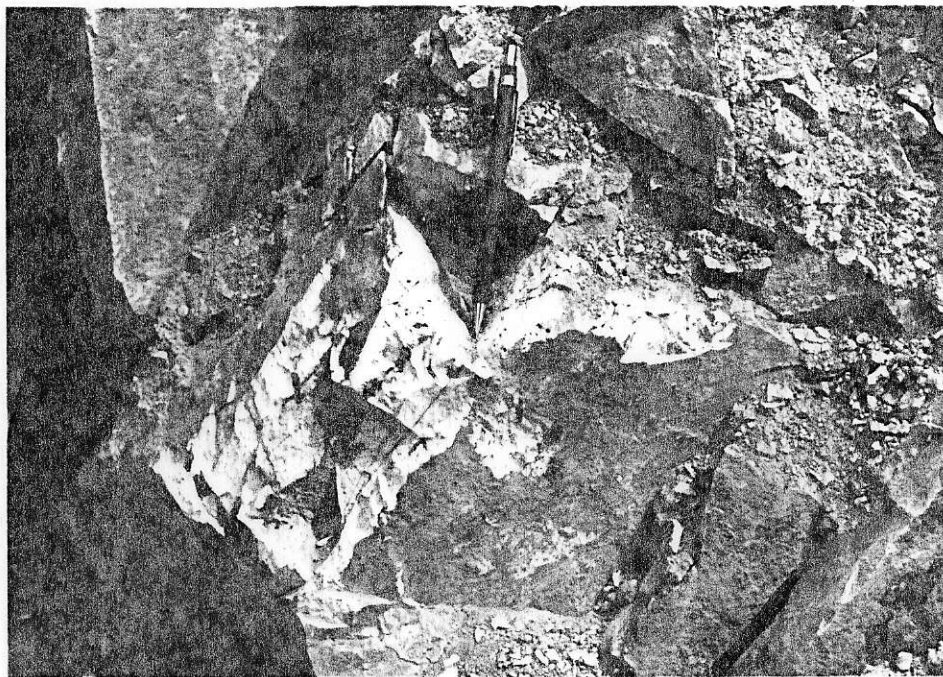


Figure 6a: Outcrop of QPP (sample site #1); quartz stockwork with and without molybdenite.



Figure 6b: QPP showing unaltered quartz and sericitized feldspar phenocrysts; molybdenite veins with ferrimolybdenite (yellow) and limonite (red-brown) coatings.

"quartz porphyry" (QPP) are host to the molybdenum mineralization.

These intrusions are easily discernable in the field because of a bleached cream colour (Figure 6a). Commonly, the rocks contain 5 to 15 per cent of 2 to 7 mm, corroded quartz eyes and sericitized plagioclase phenocrysts (Figure 6b, 7a, and 7b). The groundmass is a microgranular intergrowth of quartz, K-feldspar, and sericite. Sericitization varies from weak to complete, and the rocks are devoid of ferromagnesian gangue minerals.

Sulphides occur both in quartz (and minor quartz - K-feldspar) stockworks, and as disseminations (Figure 6b and 8). Locally, pyrite content exceeds 1 to 2 per cent, and there appears to be a barren halo in each plug (Figure 10). Some drill core samples have little or no sericite alteration and contain unaltered K-feldspar phenocrysts and only 0.1 to 0.5 per cent pyrite.

Quartz Monzonite

Only observed in drill core, the quartz monzonite (QZMZ) appears to occur in northwest-trending dyke swarms. It commonly carries less than 10 per cent feldspar phenocrysts, 2 to 4 mm in size, which have been extensively corroded and kaolinized. Primary Ti-rich biotite constitutes 3 to 5 per cent of the rock mass.

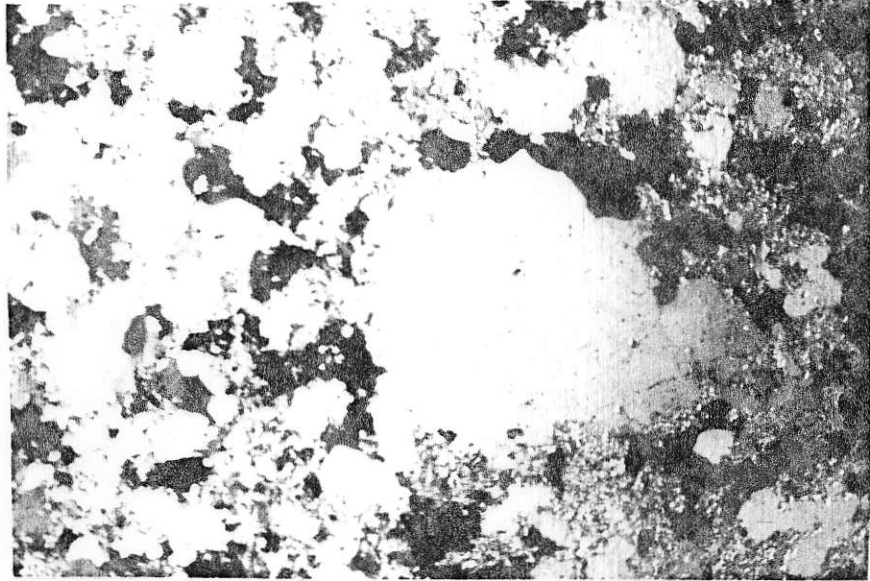


Figure 7a: Corroded, white quartz phenocrysts surrounded by a quartz-potassium feldspar-sericite (fine, bright matting) groundmass. 1.0 cm. = 0.4 mm.



Figure 7b: Magnification of a corroded interface. 1.0 cm. = 0.2 mm.

Monzonite Porphyry

A northwest-trending dyke swarm of monzonite porphyry (MZPP) incises and separates what was once a single pluton into two QPP plugs. The unit is divided into three phases: (a) "crowded" MZPP, (b) MZPP breccia, and (c) latite.

The crowded monzonite is so called because of its characteristic medium grained (1 to 5 mm), 30 to 40 per cent plagioclase, and 10 to 15 per cent biotite phenocryst content, set in fine grained (0.1 to 0.5 mm) quartz and K-feldspar groundmass. Minor kaolinization and chloritization has affected the phenocrysts.

The breccia phase comprises a crowded monzonite porphyry matrix with 5 to 40 mm angular fragments of QPP. Chalcopyrite and bornite are locally disseminated in excess of 0.5 per cent; 1 per cent pyrite is evenly disseminated throughout the rock mass.

The latite phase is characterized by 45 to 55 per cent medium to coarse grained (1 to 6 mm) K-feldspar and plagioclase phenocrysts which are moderately to completely kaolinized and sericitized, giving the rock a cream-coloured powdery appearance. Disseminated pyrite cubes, 0.5 to 3 mm in size, occupy 3 to 8 per cent of the rock mass; trace chlorite is present.



Figure 8: Fine grained, prismatic molybdenite crystals in a quartz vein. 1.0 cm. = 0.4 mm.

Hornblende-Feldspar Porphyry

A post-ore northwest-trending dyke swarm of hornblende-feldspar "porphyry" (HFP), which crosscuts both QPP and MZPP is the youngest rock unit in the map area. Relatively unaltered, 1 to 5 mm plagioclase phenocrysts constitute 40 to 45 per cent of the rock, along with 15 to 20 per cent hornblende, 1 to 3 mm in size, in a fine groundmass of feldspar, quartz, and biotite.

3.2.2 Facies and Extent of Hydrothermal Alteration

Diagnostic alteration mineral assemblages have been used to define specific alteration facies in porphyry systems (Lowell and Guilbert, 1970).

In this study only the phyllic facies was identified in the mineralized quartz porphyry. A variant of the potassic alteration facies, biotite hornfels, was observed in adjacent thermally metamorphosed Hazelton volcanics. Phyllic alteration is characterized by a quartz-sericite-pyrite assemblage. Observing the degree of sericitization of feldspar, a qualitative scale (non-weak-fair-moderate-strong-complete) was developed to assess the extent of alteration across the QPP. This interpretation, as shown in Figure 9, yields a symmetrical zoning pattern in the pluton. Correlation of the alteration zoning with the distribution of molybdenite and pyrite suggests that this exposed "horizontal" section of the pluton is within the phyllic alteration zone.

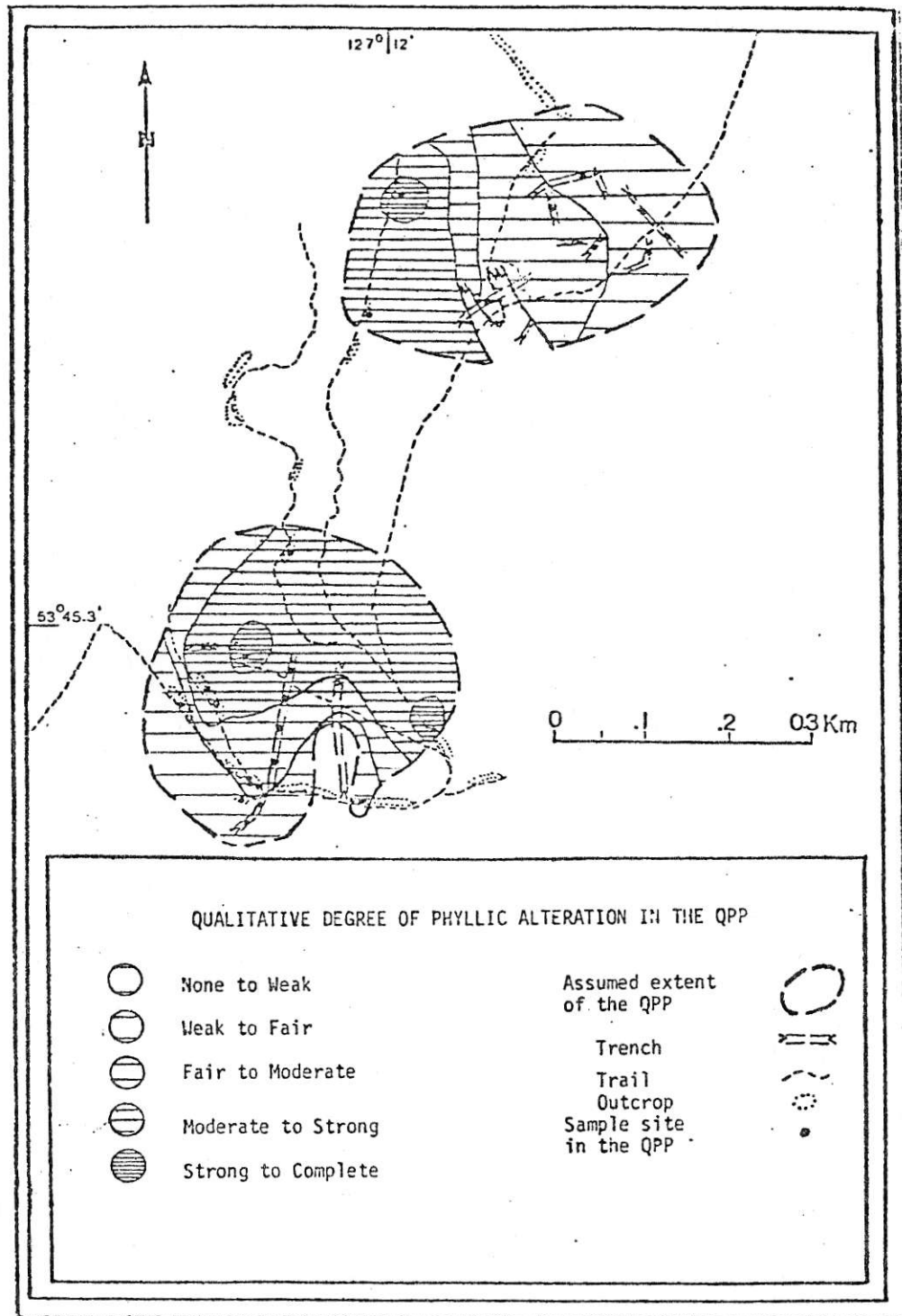


Figure 9: Qualitative degree of phyllic alteration across the quartz porphyry

Drill hole samples exhibiting none to fair sericitization, little pyrite, and unaltered K-feldspar phenocrysts, support this interpretation.

Distribution of alteration appears to be symmetrically centred between the two QPP plugs, suggesting that only one pluton was present originally and that it was later split by the intrusion of the MZPP dyke swarm.

The degree of sericitization is near-coincident with the quartz stockwork density as shown in Figure 11. Thin section studies of fine grained alteration minerals revealed distinct differences in optical characteristics. Sericite (a fine grained white mica) is readily identified by its third order red-blue-green interference colours. Kaolinite (a clay mineral) has a first order white-cream interference colour.

Supergene alteration has resulted in weak limonitic staining and the formation of yellow ferrimolybdate ($\text{Fe}_2(\text{MoO}_4)_3 \cdot 8\text{H}_2\text{O}$) along molybdenite-rich veins (Figure 6b).

3.2.3 Sulphide Mineralogy

There are two types of metallized zones; a Mo zone in the QPP where the fine grained molybdenite is fracture-controlled, and a zone of disseminated copper sulphides (with anomalous trace zinc values) in the MZPP unit (Figure 10).

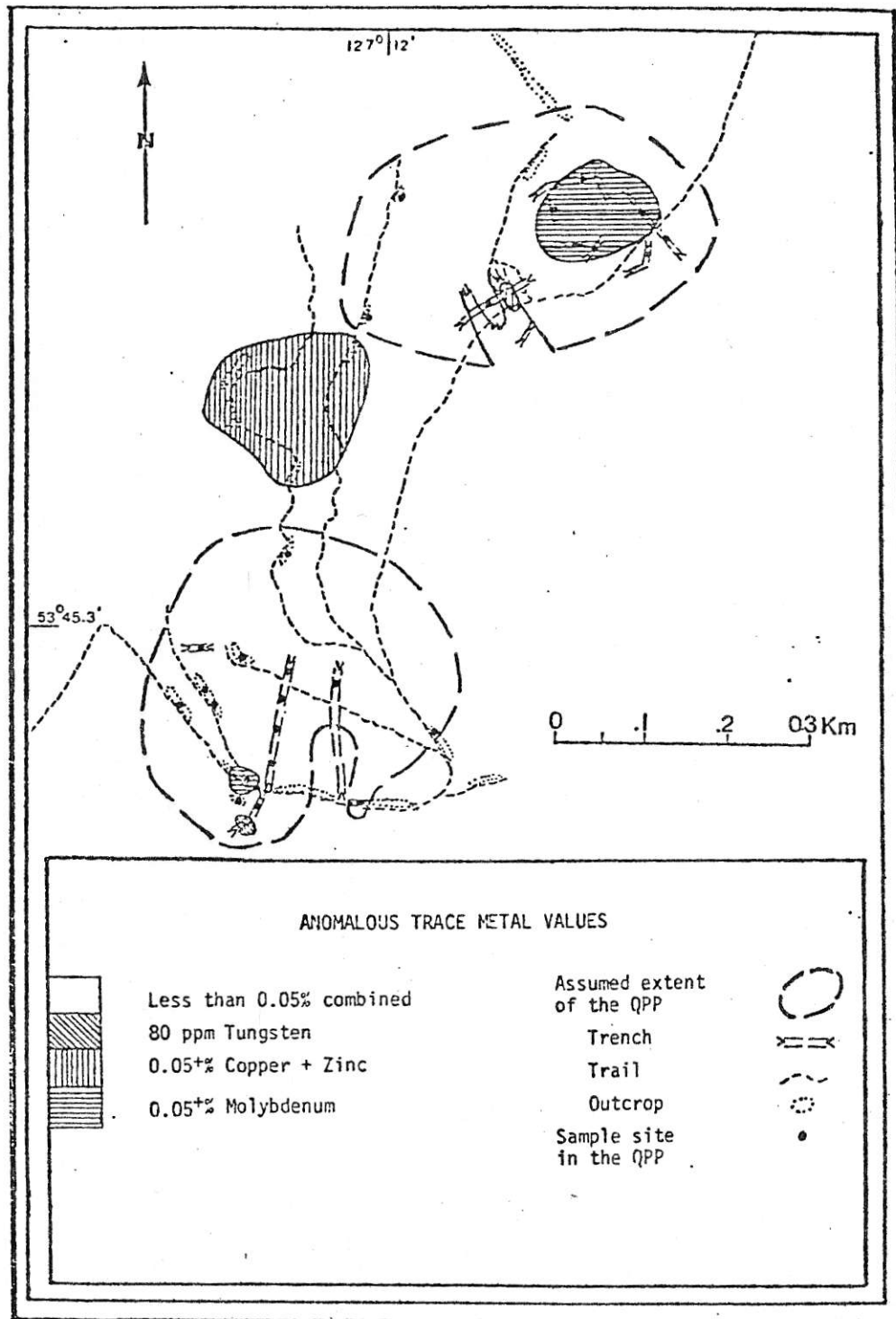


Figure 10: Metalliferous zones

Pyrite is the most abundant sulphide mineral and occurs as disseminations throughout all the lithologies in the map area, and as fracture fillings and in quartz veins in the QPP and the older surrounding units. Molybdenite occurs as fracture fillings and in quartz stockworks where sericitization and stockwork development are fair to moderate. Disseminated chalcopyrite and bornite are observed in the MZPP.

Molybdenite grades averaged over long drill intercepts indicate the presence of approximately 40,000,000 tonnes of 0.06 per cent molybdenite.

CHAPTER 4 - CHEMISTRY OF THE DEPOSIT

Major, minor, and trace element content of the QPP was investigated in order to:

- (1) relate zoning patterns of major oxides and trace elements to hydrothermal alteration and mineralization;
- (2) chemically identify highly altered and weathered rocks;
- (3) define a suitable model of magma genesis and classify the type of deposit based on characteristic chemical features.

Major oxide analyses by X-ray fluorescence (XRF) on thirty-three rock samples were performed by the Geological Survey of Canada (GSC) Analytical Chemistry Laboratory. Data is tabulated in Appendix I. The calculated mean composition of the QPP and the precision of the analyses, based on six control XRF and a control total dissolution HF/HClO₄/HNO₃ analysis, are listed in Appendix II.

Minor and trace element analyses by atomic absorption spectrometry (AAS) were performed on the same thirty-three samples. Data is listed in Appendix III. Precision calculations based on six control AAS analyses are given in Appendix IV.

Normative quartz-albite-orthoclase compositions were computed using a GSC norm calculation programme. Programme parameters along with norm ratios for the QPP are listed in Appendix V.

4.1 Chemical Zonation within the Quartz Porphyry

Major Element Chemistry:

Major element analyses show that the QPP is a silica- and potassium-rich, peraluminous rock, depleted in Ca, Na, Ti, Mn, total Fe, and Mg. The GSC norm calculation programme classifies the QPP as a silicified, K-rich granite (Figure 12).

Although relatively unaltered rocks were preferred for chemical analysis, apparently no rocks have escaped hydrothermal and/or supergene alteration. Major element analyses of the least silicified specimens (less than 78 weight per cent SiO_2) were inconsistent with each other (that is they had erratic values of Al_2O_3 , TiO_2 , MgO , and total Fe). Hence, the chemistry of the QPP referred to in this paper will be the mean composition of all analyses and will only be compared with literature analyses of similarly altered plutons. Average weight percentages of the major oxides are: $\text{SiO}_2 = 80.1$, $\text{K}_2\text{O} = 4.3$, and $\text{Al}_2\text{O}_3 = 11.4$. Variation plots of these oxides, across the QPP, are given in Figures 11, 13, and 14.

The average alkali ratio $\text{K}_2\text{O}/\text{Na}_2\text{O}$ is 26.9. There is no correlation between soda-content and K_2O , SiO_2 , or

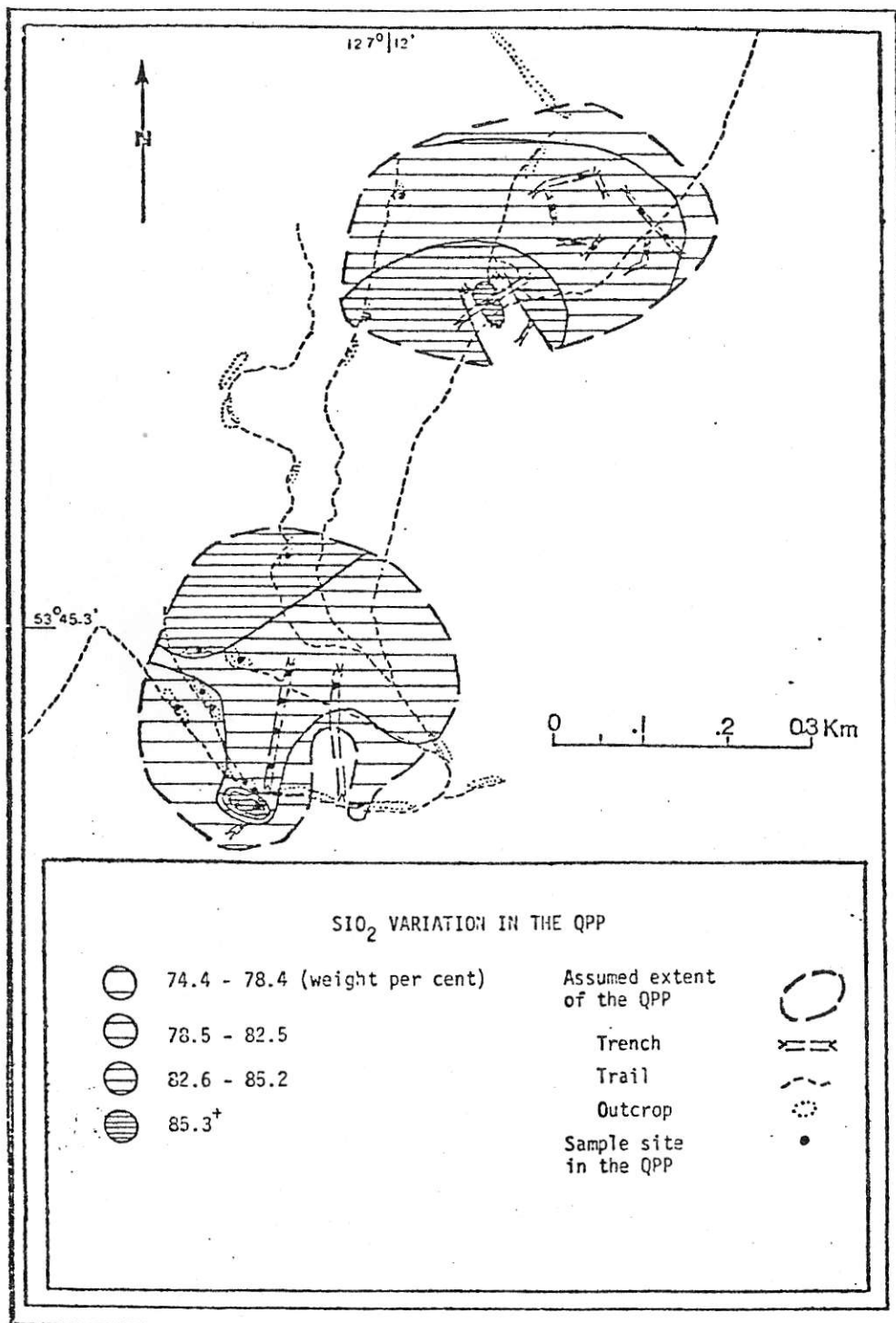


Figure 11: Variation of SiO₂ (weight per cent) across the QPP

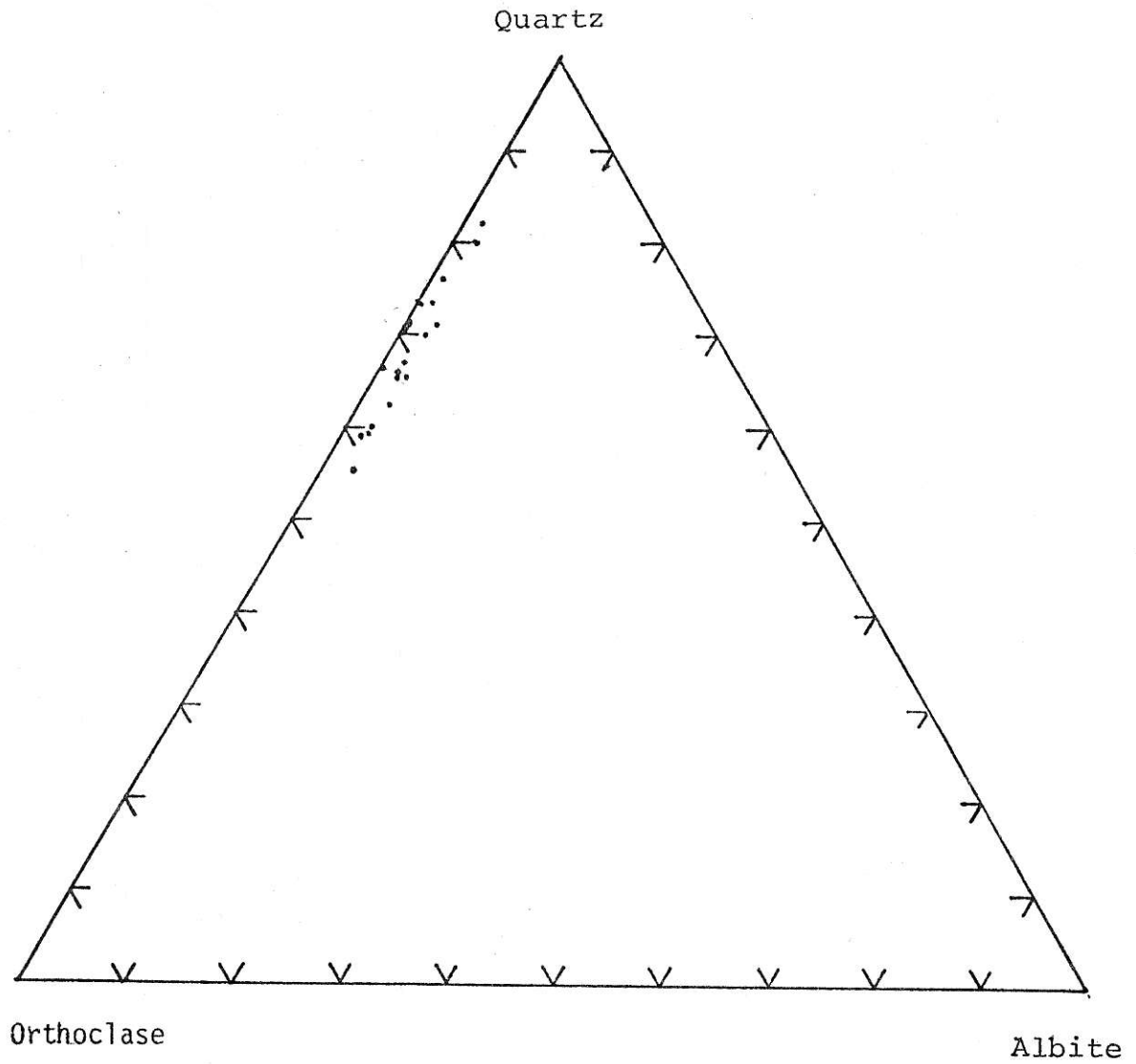


Figure 12:
Ternary plot of normative quartz-albite-orthoclase
ratios of the QPP.

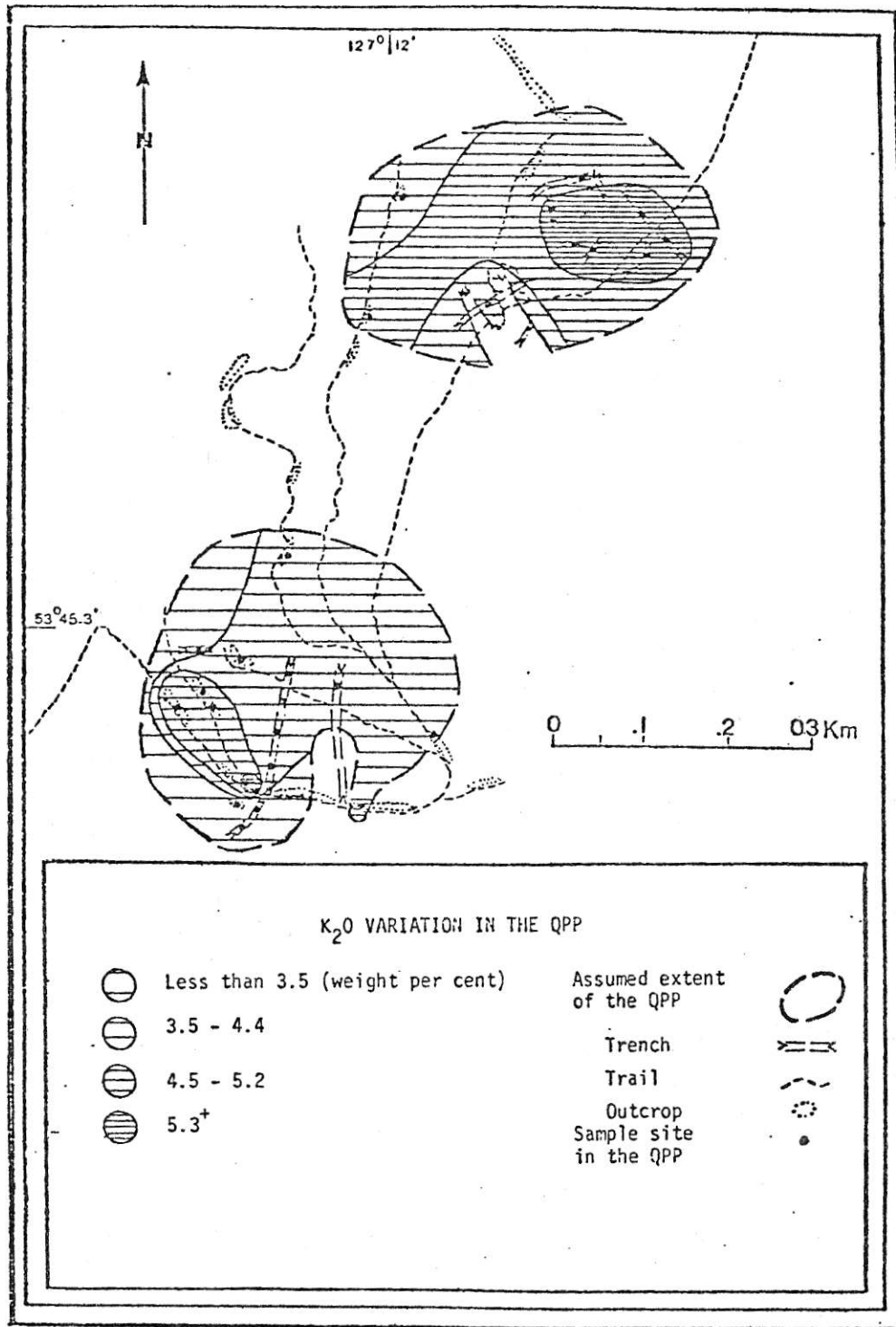


Figure 13: Variation of K₂O (weight per cent) across the QPP²

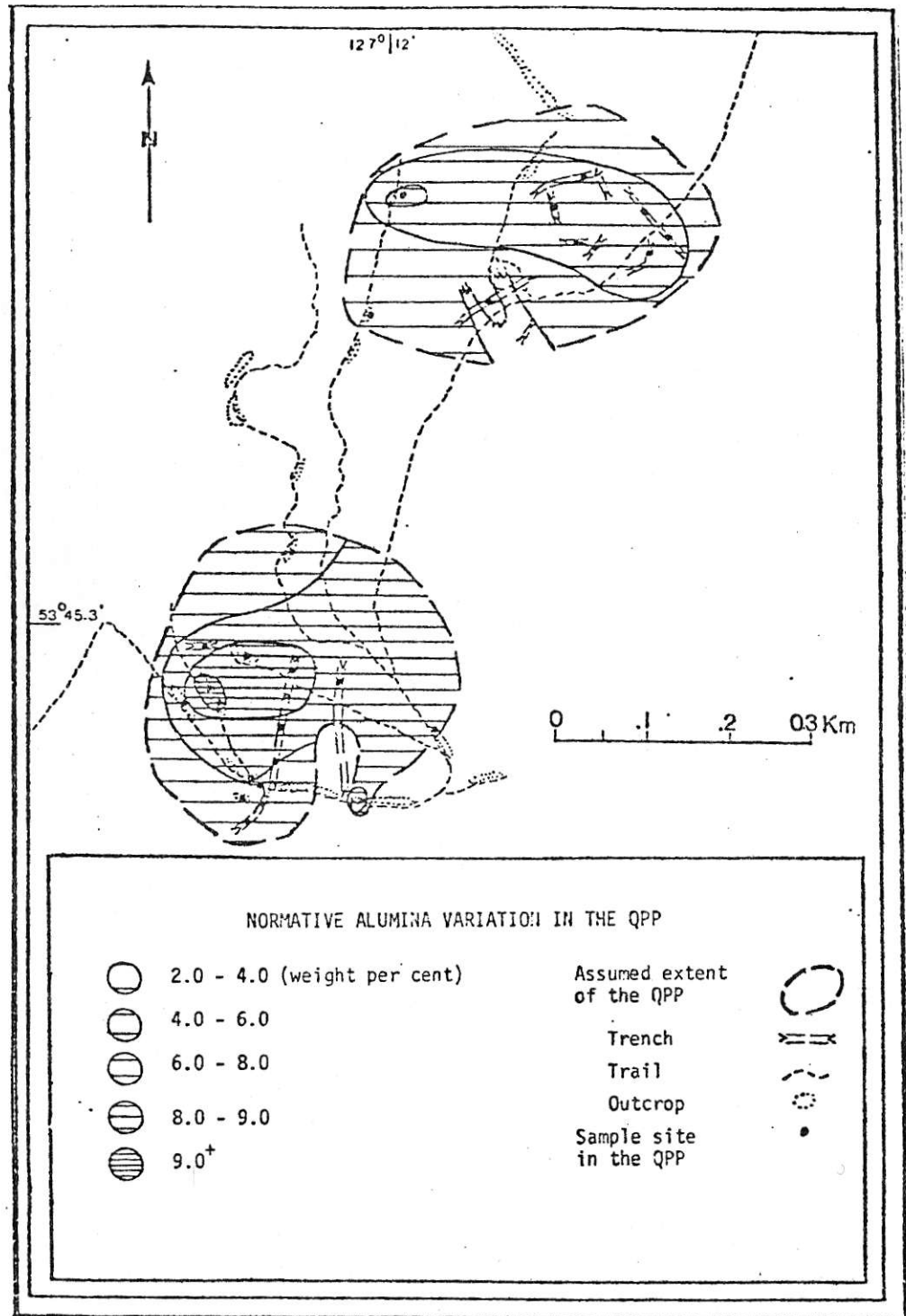


Figure 14: Variation of normative corundum across the QPP

degree of alteration. Enrichment of rubidium with respect to strontium is suggested by the "positive" ratio of Rb/Sr being 1.64.

Minor Element Chemistry:

Minor element analyses yield the distribution of the ore metals. The average molybdenum, tungsten, and copper contents of the QPP are 0.022, 0.002, and 0.002 per cent respectively. Anomalous zones of greater than 0.05 per cent molybdenum, 0.05 per cent copper, and 80 ppm tungsten, are shown in Figure 10. Anomalous zinc values occur with the copper. The average Mo to Cu ratio of the QPP is 10.9.

Fluorine content in the QPP averages 0.04 per cent and as shown in Figure 15, fluorine concentration coincides with that of molybdenum and potassium.

4.2 Effect and Similarity Between Alteration, Mineralization, and Chemistry

Relationships between the chemistry of the QPP and the alteration can be indicative of the processes of magma generation and emplacement.

The effects of hydrothermal processes are highly dependent upon the chemistry of the fluids involved. Both the chemistry and the degree of alteration is semi-symmetrically zoned, rather than erratic. Some plots show similar zonation patterns centred between the two plugs, further

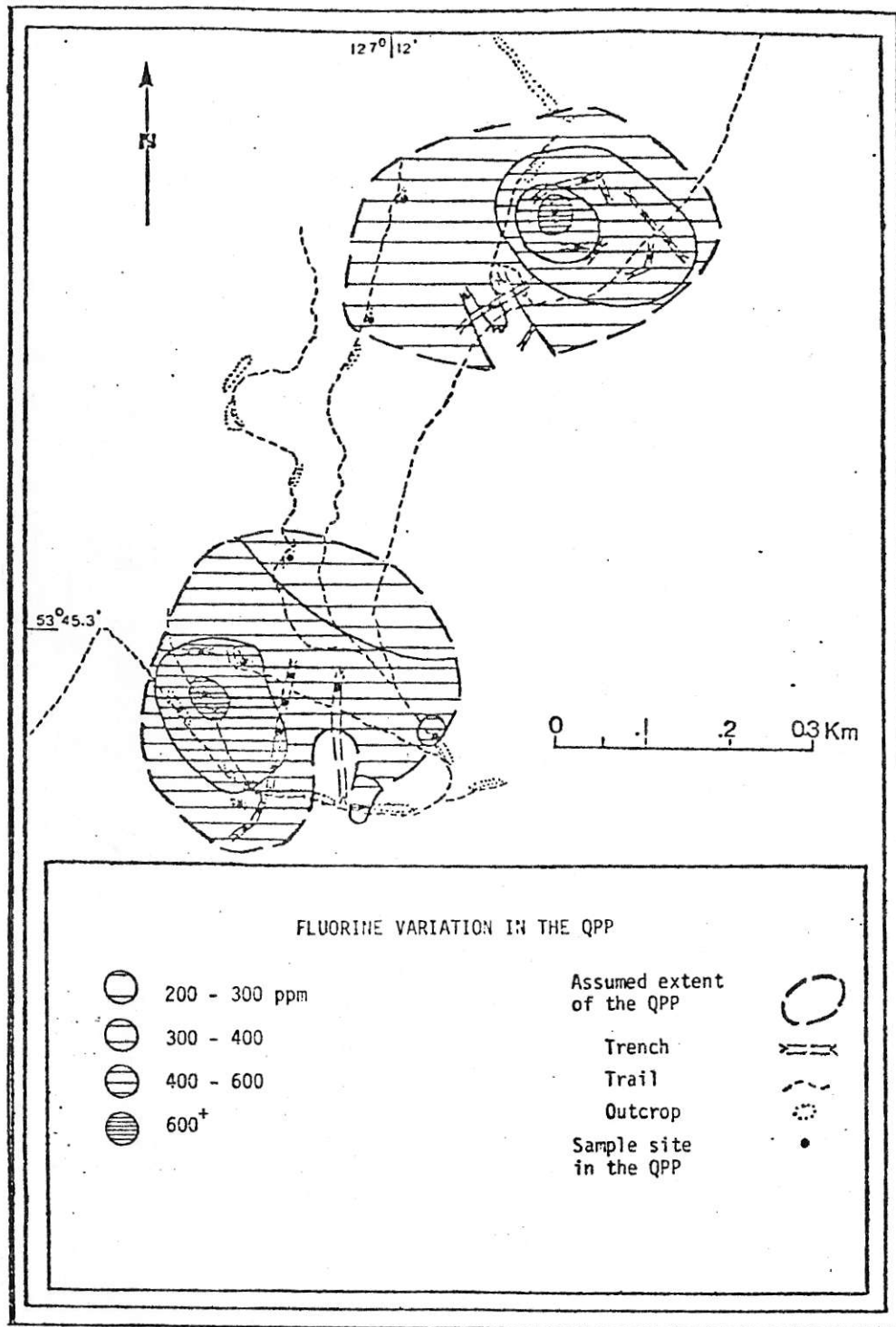


Figure 15: Variation of fluorine (parts per million) across the QPP

suggesting that the QPP plugs were originally a single pluton. The qualitative degree of quartz-sericite-quartz alteration exhibits such a tendency. The SiO_2 zonation reflects the degree of development of the quartz stockwork. Local compositions exceed 76 per cent normative quartz (Sample 7).

Two mineralized centres, one in each plug, are represented by the Mo, K_2O , normative Al_2O_3 , and F content of the QPP. These centres are in areas of weak to moderate phyllic alteration and quartz stockwork development.

Comparison of the chemistry of the various "differentiates" of the Bulkley intrusions yields a few characteristic features (Table 2). The QPP has an average normative quartz and corundum content of 64 and 6.6 per cent respectively. This is compared with values of less than 30 and 3.0 per cent respectively, for all the other intrusive phases. The average ratio of orthoclase to albite for the QPP is 15:1, compared with 1:1 to 1:2 for the other intrusives. The average ratio of Rb to Sr is 1.6:1 for the QPP but 1:2 to 1:12 for the other rocks.

4.3 Summary

The "QPP" is an altered granitic rock characterized by enrichment of SiO_2 , Al_2O_3 , and K_2O , and depletion of Na_2O , CaO , TiO_2 , MnO , total Fe, and MgO . There is an anomalous enrichment of F, Rb, Mo, and W with respect to Sr and Cu.

Intensity of phyllic alteration is not related directly

TABLE 2 - WHOLE ROCK ANALYSES OF BULKLEY INTRUSIONS

	<u>GRDR</u> ¹	<u>QPP</u> ²	<u>MZPP</u> ³	<u>HFP</u> ⁴
Weight per cent				
SiO ₂	65.2	80.1	65.7	62.7
TiO ₂	.51	.14	.53	.66
Al ₂ O ₃	15.8	11.4	15.6	16.7
Fe ⁵	4.2	1.3	3.9	5.3
MgO	1.8	.31	1.8	2.5
CaO	2.8	.09	2.1	3.2
Na ₂ O	3.2	.16	3.1	3.4
K ₂ O	3.6	4.3	3.4	2.7
Parts per million				
Rb	70	84	90	70
SR	350	51	430	500
Mo	3	218	8	4
Cu-Zn	301	34 ⁶	608	134
W	3	20	4	2
F	380	370	400	420

1. Granodiorite, 2 analyses
2. Quartz porphyry, 19 analyses
3. Monzonite porphyry, 5 analyses
4. Hornblende-feldspar porphyry, 3 analyses
5. Total fe content = Fe₂O₃ + FeO
6. Cu = 20 ppm, Zn = 14 ppm

to either the degree of quartz stockwork development or mineralization. There appears to be direct correlations between K_2O , F, and Mo concentration. Normative corundum content is unrelated to the degree of alteration, suggesting that the original melt was peraluminous.

Lithogeochemical zoning supports the possibility that there was originally a single pluton, bisected by a younger intrusion, rather than two separate plugs representing separate apophyses of a larger pluton at depth. In the latter case, chemical trends would more likely show a closed zoning pattern within each plug. However, the zoning patterns tend to be open.

On the other hand, variations of Mo, K_2O , F and Al_2O_3 suggest two centres of mineralization. Multiple phases of mineralization may possibly explain the presence of more than one molybdenite zone.

Ratios of Rb to Sr suggest different source material for the QPP and all other intrusive phases.

CHAPTER 5 - GENESIS AND CLASSIFICATION OF STOCKWORK MOLYBDENUM DEPOSITS

5.1 General Description

Stockwork molybdenum deposits are commonly referred to as "porphyry-type" deposits because of similarities with their copper-rich counterparts. Both are genetically related to intrusive granitic bodies which were emplaced at a shallow depth. Hydrothermal processes of ore deposition and alteration are similar in that mineralization and alteration patterns often reflect the shape of the intrusion. Tectonic settings of the deposits and chemistry of the associated intrusions, relate magma and ore genesis to processes of subduction and rifting. Recently, important differences in magma series chemistry have justified separate classifications for stockwork molybdenum deposits (Mutschler, et al, 1981; Westra and Keith, 1981; White, et al, 1981; Sillitoe, 1980; Woodcock and Hollister, 1978; Soregaroli and Sutherland Brown, 1976).

Stockwork (porphyry) molybdenite deposits are characterized by mineralization dispersed chiefly in veinlet and fracture stockworks with or without quartz or pyrite. Molybdenite grain size is generally less than 1 millimetre. Related intrusions of acid to intermediate composition commonly exhibit a porphyritic texture with an aphanitic matrix.

Important differences between Mo and Cu-Mo porphyry-type deposits lie in the rock chemistry. Presence of fluorine-bearing minerals, lithophile elements such as Li, Sn, W, Ta, U, Th, Y, and trace elements Rb and Nb, characterize stockwork molybdenum deposits.

Processes of element concentration by convection-driven thermogravitational diffusion can generate high silica, volatile-rich melts common to Mo deposits (Mutschler, 1981). These processes are conducive to enrichment of magma in lithophile elements and depletion in Ti, total Fe, Mg, and Sr.

In molybdenite systems a direct correlation often appears between Mo, K, and F content. Westra and Keith (1981) show that the load capacity of a volatile-rich melt for Mo is increased with increasing K and F content. This load capacity increases for Sn, W, and Ta as well. It was also shown (previous citation) that a close correlation exists between K and F content and the depth to the Benioff zone.

Stockwork Mo deposits are classified initially on silica and alkali content. More detailed study shows that each "deposit-type" has its characteristic trace element chemistry. To explain the trace chemistry and global setting of the deposits, tectonic magma genesis models have been assigned to each deposit-type. The most common deposits are the "calc-alkaline" Mo deposits (stock and plutonic types - depending on pluton size, shape, and

depth of emplacement) and the "alkali-calcic" Mo deposits (Climax-type).

Calc-alkaline stockwork Mo and porphyry Cu deposits occupy similar positions within magmatic arcs. Westra and Keith (1981) suggest a continuum exists between Mo deposit endmembers (Endako), through Mo-Cu deposits to Mo-rich porphyry Cu deposits (Brenda). No such continuum exists between Climax-type Mo and porphyry Cu deposits. Some molybdenum deposits appear transitional between the calc-alkaline and Climax-types (Questa, Mount Hope, Glacier Gulch).

5.2 Whiting Creek

General characteristics (Westra and Keith, 1981) of setting, petrography, and chemistry of calc-alkaline and Climax-type stockwork molybdenum deposits, are given in Table 3. The features listed for Whiting Creek are average values for the altered QPP.

Important similarities between Whiting Creek and the Climax-type are the cogenetic granite rock type, major oxide content, "positive" (greater than one) Rb to Sr ratio and the trace element assemblage Mo-F-(W).

Major, minor, and trace concentrations appear slightly lower than those values quoted for unaltered rocks by Westra and Keith (1981). Slight depletion due to hydrothermal and supergene alteration may explain these values. Lower K_2O and trace concentrations, regional tectonic setting

TABLE 3 - GENERAL CHARACTERISTICS OF STOCKWORK
MOLYBDENUM DEPOSITS

	Calc-alkaline ¹ Stock and Plutonic type	Alkali-Calcic ¹ Climax-type	Whiting Creek ²
Geotectonic Setting	Compressive Continental Plate Margin	Subduction-related continental back-arc spreading environment	Continental volcanic arc regime with possible local rifting
Cogenetic igneous rocks	Quartz monzon- ite Granodiorite	Rhyolite Granite	Granite
Porphyry texture	Yes and no	Yes	Yes
SiO ₂ %	70	75	80
K ₂ O %	4	5	4.3
TiO ₂ %	0.1 - 0.2	0.2	0.14
F %	0.1 - 0.25	0.5 - 2	0.04
Rb ppm	100 - 350	200 - 800	84
Sr ppm	100 - 800	125	51
Rb/Sr	1	1	1.64
F/Cl	low	high	?
Nb ppm	20	25 - 200	?
Important elements	Mo-Cu-(W)	Mo-F-W-Sn	Mo-F-(W)
Multiple ore shells	No	Common	?
Max. Mo con- tent in million tons	0.3 - 1.6	2.0	*
MoS ₂ % in ore zone	0.1 - 0.25	0.2 - 0.49	*
Examples	Kitsault Endako	Climax Urad-Henderson Mount Hope ⁴ Glacier Gulch ⁴	

1. Relatively unaltered rocks (Westra and Keith, 1981)
2. Altered quartz porphyry
3. D.G. MacIntyre (1976)
4. Climax transitional-type
- * Presently undefined

and low grade and tonnage figures are similar to those of the calc-alkaline type.

A Climax "transitional-type" deposit has been suggested for Climax-type deposits having characteristics similar to the calc-alkaline type. The Whiting Creek deposit has been suggested to be of this type primarily because of the chemistry of the cogenetic igneous rocks.

Chemical analyses of altered granite rocks from a Climax- and transitional-type deposit are listed in comparison to the mean composition of the altered QPP, in Table 4.

TABLE 4 - CHEMICAL ANALYSES OF ALTERED GRANITE ROCKS

	1	2	3
	<u>Climax</u> <u>type</u>	<u>Transitional</u> <u>type</u>	<u>Whiting</u> <u>Creek</u>
Weight per cent			
SiO ₂	77.50	77.10	80.07
Al ₂ O ₃	10.10	11.30	11.42
Fe ₂ O ₃	0.86	0.20	0.50
FeO	0.26	0.30	0.84
MgO	0.07	0.50	0.31
MnO	N.A.	0.01	0.01
CaO	0.40	0.50	0.09
Na ₂ O	0.31	0.60	0.16
K ₂ O	7.30	8.60	4.26
TiO ₂	0.38	0.04	0.14
Parts per million			
Rb	550	N.A.	84
Sr	140	N.A.	51
F	N.A.	400	370

1. Southwest mass of Climax stock - potassic and phyllic alteration Climax Colorado (White, et al, 1981)
2. Strongly altered rhyolite porphyry, Mount Hope, Nevada (Mutschler, et al, 1981)
3. Quartz-sericite alteration, quartz porphyry, Whiting Creek, British Columbia

CHAPTER 6 - CONCLUSIONS

The petrography and setting of the Whiting Creek occurrence are consistent with the interpretation that it is a stockwork molybdenum deposit. Whole rock and trace chemistry suggest a "Climax transitional-type" molybdenum deposit. The supporting features for such a model are:

- (1) The lithologies and their interstructural relations are conducive to the models of an initial volcanic island arc regime being followed by a continental volcanic arc regime with possible local rifting. This geotectonic setting is, in part, a fundamental requirement in the genesis of stockwork molybdenum deposits (Sillitoe, 1980).
- (2) Whiting Creek, located in the Intermontane belt of the Cordillera and of late Cretaceous age, is coincident in formation with a large group of known porphyry-type deposits.
- (3) The molybdenite mineralization is principally veinlet- and fracture-controlled.
- (4) Effects of hydrothermal processes to yield characteristic alteration and mineralization patterns. This is shown by a characteristic quartz-sericite-pyrite (phyllic) alteration assemblage in which the Mo-rich quartz stockwork is developed.
- (5) The mineralized pluton exhibits a porphyritic texture with an aphanitic matrix.

- (6) Characteristic oxides supporting the Climax-type model are given by the following average contents (by weight per cent); $\text{SiO}_2 = 80.6$, $\text{K}_2\text{O} = 4.3$, and $\text{TiO}_2 = 0.14$.
- (7) Characteristic traces supporting the Climax-type model are the average ratios of $\text{Mo/Cu} = 10.9$ and $\text{Rb/Sr} = 1.64$.
- (8) The average F content of 0.04 per cent is in agreement with those values quoted for strongly altered Climax-type plutons (Mutschler, et al, 1981).
- (9) The relationship between K, F, and Mo enrichment, supports the Climax-type element concentration model of thermogravitational diffusion.
- (10) The Glacier Gulch Mo deposit, Smithers, British Columbia, is considered by Westra and Keith (1981) to be a Climax transitional-type stockwork deposit. This deposit, situated 100 km due north of Whiting Creek, is set in an early rhyolitic plug which has been crosscut by monzonitic intrusions. These rocks are part of the Bulkley intrusions.

The similarities in the lithologies, chemistry, and geotectonic setting between Glacier Gulch and Whiting Creek, imply that possibly these two deposits were formed by very similar processes and that there are potentially more deposits of this kind to be found in the Canadian Cordillera.

Identification of possible source material and hydrothermal fluid composition, through isotope and fluid inclusion studies, may clarify the deposit type. Trace analyses on Sn, Nb, and Cl, would also yield characteristic traits on magma genesis.

Mineralogical and textural evidence of the presence of a core potassic alteration zone was not observed. The degree of phyllic alteration and lack of an extensive barren pyritic halo suggests proximity to the core of the hydrothermal system.

If this is the centre of the system, then it is likely that the hydrothermal event was too weak to produce the potassic zone and associated mineralization.

However, the alteration and mineralization might be the result of a late-stage event. This would imply that there might exist a much larger deposit at depth which may be offset by faulting.

Lithochemistry suggests that potassium and fluorine may be used as pathfinder elements for molybdenum. However, before these chemical trends can be used authoritatively, sample density should be increased and vertical zonation patterns studied.

REFERENCES

- Bright, J.M. and Jonson, D.C., 1976, Glacier Gulch (Yorke-Hardy); in Porphyry Deposits of the Canadian Cordillera, Sutherland Brown, A., ed., CIMM Spec. Vol.15, p.455-461.
- Cann, R.M., 1982, Geological Map of Whiting Creek (WHIT 1-6); SMD Mining Co. Ltd. Map.
- Carter, N.C., 1974, Geology and geochronology of porphyry copper and molybdenum deposits in west-central British Columbia; unpublished Ph.D. thesis, University of British Columbia, Vancouver.
- Duffell, S., 1959, Whitesail Lake Map-area, British Columbia; Geol.Surv.Can. Mem. 299, 119p.
- Godwin, C.I., 1975, Imbricate subduction zones and their relationship with upper Cretaceous to Tertiary porphyry deposits in the Canadian Cordillera; Can. J. Earth Sci., v.12, p.1362-1378.
- Guilbert, J.M. and Lowell, J.D., 1974, Variations in zoning patterns in porphyry ore deposits; CIMM Bull. v.67, p.99-109.
- Hedley, M.S., 1935, Tahtsa-Morice Area, Coast District, British Columbia; Geol.Surv.Can. Map 367A.
- Hollister, V.F., 1975, An appraisal of the nature and source of porphyry copper deposits; Minerals Sci. Engng., v.7-3, p.225-233.
- Lowell, J.D. and Guilbert, J.M., 1970, Lateral and vertical alteration - mineralization zoning in porphyry ore deposits; Econ. Geol., v.65, p.373-408.
- MacIntyre D.G., 1976, Evolution of upper Cretaceous volcanic and plutonic centres and associated porphyry copper occurrences, Tahtsa Lake area, British Columbia; Unpublished Ph.D. thesis, University of Western Ontario, London.
- MacIntyre, D.G. and Hodder, R.W., 1978, Place and time of porphyry-type Cu-Mo mineralization in upper Cretaceous caldera development, Tahtsa Lake, British Columbia; Fifth Quadrennial IAGOD Symposium, Utah, Proceedings Vol.1, p.175-183.

- McMillan, W.J. and Panteleyev, A., 1980, Ore deposit models -1. Porphyry copper deposits; Geoscience Canada, v.7-2, p.52-63.
- Mutschler, F.E., Wright, E.G., Ludington, S. and Abbott, J.T., 1981, Granite Molybdenite Systems; Econ.Geol., v.76, p.874-897.
- Panteleyev, A., 1981, Berg porphyry Cu-Mo deposit: geological setting, mineralization, zoning and pyrite geochemistry; British Columbia MEMPR Bull.66, 158p.
- Sillitoe, R.H., 1980, Types of porphyry molybdenum deposits; Mining Magazine, June, p.550-553.
- Soregaroli, A.E. and Sutherland Brown, A., 1976, Characteristics of Canadian Cordilleran molybdenum deposits; in Porphyry deposits of the Canadian Cordillera, Sutherland Brown, A., ed., CIMM, Spec. Vol.15, p.417-431.
- Sutherland Brown, A., 1976, Porphyry deposits of the Canadian Cordillera, CIMM Spec. Vol.15, 510p.
- Titley, S.R. and Beane, R.E., 1981, Porphyry copper deposits; Econ. Geol., Seventy-Fifth Anniv. Vol., p.214-269.
- Westra, G. and Keith, S.B., 1981, Classification and genesis of stockwork molybdenum deposits; Econ. Geol., v.76, p.844-873.
- White, W.H., Bookstrom, A.A., Kamilli, R.J., Gangster, M.W., Smith, R.P., Ranta, D.E. and Stininger, R.C., 1981, Character and origin of Climax-type molybdenum deposits; Econ. Geol., Seventy-Fifth Anniv. Vol., p.270-316.
- Woodcock, J.R. and Hollister, V.F., 1978, Porphyry molybdenite deposits of the North American Cordillera; Minerals Sci. Engng., v.10-1, p.3-18.

APPENDIX I

Major and minor element analyses - by XRF

<u>Sample Number</u>	<u>Rock Type</u>	<u>SiO₂ %</u>	<u>TiO₂ %</u>	<u>Al₂O₃ %</u>	<u>Total FE %</u>	<u>MgO %</u>	<u>CaO %</u>	<u>Na₂O %</u>	<u>K₂O %</u>	<u>Rb ppm</u>	<u>Sr ppm</u>
01	QPP	79.4	0.09	12.0	1.2	0.30	0.08	0.2	4.59	90	50
02	QPP	76.6	0.13	13.4	1.6	0.19	0.08	0.3	5.93	110	50
04	QPP	82.7	0.09	11.5	0.6	0.19	0.08	0.1	3.26	70	30
05	HFP	61.2	0.64	17.5	5.0	2.83	3.54	3.2	2.41	80	490
06	QPP	78.4	0.09	12.8	1.2	0.46	0.11	0.2	4.52	90	40
07	QPP	85.3	0.14	8.8	0.9	0.29	0.12	0.2	2.32	40	60
09	QPP	86.0	0.13	7.8	0.9	0.38	0.10	0.2	2.61	40	50
10	QPP	80.6	0.09	10.8	1.5	0.31	0.10	0.0	3.70	80	50
11	QPP	79.8	0.09	12.6	1.3	0.29	0.07	0.1	3.54	90	50
12	MZPP	66.9	0.51	15.3	3.8	1.60	2.41	2.9	3.35	210	470
13	QPP	82.5	0.09	9.5	1.1	0.21	0.13	0.3	4.73	80	50
14	QPP	81.4	0.09	11.4	0.7	0.14	0.08	0.0	4.03	60	40
15	QPP	78.2	0.11	11.7	1.7	0.31	0.10	0.2	5.53	90	50
16	QPP	78.6	0.10	11.4	1.9	0.27	0.09	0.3	4.88	90	40
18	QPP	86.0	0.08	7.4	0.7	0.24	0.09	0.3	3.89	70	70
19	MZPP	66.2	0.53	15.9	4.0	1.72	2.79	3.4	2.94	30	510
21	QPP	77.1	0.11	12.0	2.0	0.34	0.10	0.2	5.38	110	30
22	QPP	78.9	0.12	13.1	0.7	0.37	0.09	0.0	4.12	100	30
23	QPP	81.3	0.08	11.8	0.6	0.11	0.07	0.2	4.53	80	60
24	CRDR	65.4	0.51	15.7	4.2	1.83	2.53	3.0	4.13	100	320
25	QPP	79.0	0.25	12.2	1.2	0.34	0.09	0.2	3.83	80	80
27	HFP	65.2	0.61	16.3	4.1	2.06	2.66	4.1	2.84	70	520
28	CRDR	65.0	0.51	15.9	4.3	1.75	3.09	3.3	3.08	40	390
29	QPP	74.4	0.40	13.5	3.0	0.44	0.09	0.0	4.41	110	50
30	HFP	61.7	0.73	16.2	6.4	2.48	3.41	2.9	3.80	70	500
31	MZPP	64.6	0.49	15.7	3.9	1.86	1.63	3.4	3.28	50	450
32	MZPP	63.9	0.63	16.1	4.4	2.18	2.14	3.3	2.82	80	490
33	QPP	83.1	0.08	9.3	1.0	0.22	0.09	0.0	4.22	60	80
37	MZPP	67.1	0.50	15.0	3.4	1.78	1.37	2.6	4.49	80	220

Analysis of samples 03, 08, 35, 36 considered invalid due to contamination.

APPENDIX II

Mean and standard deviation values of whole rock analyses on the control sample and QPP.

<u>Analysis</u>	<u>Number of Samples</u>		<u>SiO₂</u>	<u>TiO₂</u>	<u>Al₂O₃</u>	<u>Total Fe</u>	<u>MgO</u>	<u>CaO</u>	<u>Na₂O</u>	<u>K₂O</u>
			Weight per cent							
XRF	6	mean	63.8	0.42	16.7	3.00	2.00	3.48	3.4	3.49
		std.dev.	0.4	0.0	0.1	0.1	0.04	0.03	0.1	0.02
Total Dissolution HF/HClO ₄ /HNO ₃	1		63.96	0.40	16.57	3.03	1.84	2.98	3.80	3.43
XRF	19 x QPP	mean	80.07	0.14	11.42	1.34	0.31	0.09	0.16	4.26
		std.dev.	3.65	0.09	1.99	1.23	0.15	0.02	0.11	0.91

Good precision and accuracy indicated by comparison of XRF and total dissolution analyses results.

APPENDIX III

Trace element analyses - by AAS

<u>Sample Number</u>	<u>Rock Type</u>	<u>Zn</u>	<u>Cu</u>	<u>Mo</u>	<u>W</u>	<u>F</u>
Parts per million						
01	QPP	11.6	12	108	16	410
02	QPP	12.1	14	56	4	330
03	QPP	14.9	25	27	20	680
04	QPP	15.6	6	76	8	410
05	HFP	53.5	40	5	1	410
06	QPP	10.6	10	80	16	410
07	QPP	16.6	10	154	8	330
08	QPP	14.2	26	4	80	330
09	QPP	11.9	10	27	8	330
10	QPP	7.9	9	286	24	410
11	QPP	7.4	19	61	16	380
12	MZPP	88.0	1380	4	1	440
13	QPP	13.3	67	36	4	220
14	QPP	22.8	17	40	8	250
15	QPP	9.0	20	407	24	330
16	QPP	36.9	42	862	24	330
18	QPP	12.0	27	865	20	220
19	MZPP	54.8	124	3	1	330
21	QPP	14.7	24	500	1	760
22	QPP	14.3	9	70	16	410
23	QPP	10.9	9	569	24	300
24	GRDR	37.0	420	1	1	380
25	QPP	11.5	13	33	12	410
27	HFP	61.1	60	5	4	440
28	GRDR	45.6	99	5	1	380
29	QPP	15.1	41	44	32	250
30	HFP	50.0	137	3	1	410
31	MZPP	28.0	438	9	4	410
32	MZPP	54.8	223	17	1	500
33	QPP	9.9	15	55	4	220
35	QPP	22.7	90	4	20	250
36	MZPP	22.1	48	137	16	200
37	MZPP	64.7	584	138	12	330

APPENDIX IV

Mean and standard deviation values of trace element analyses of the control sample and QPP.

<u>Analysis</u>	<u>Number of Samples</u>		<u>Zn</u>	<u>Cu</u>	<u>Pb</u>	<u>Mo</u>	<u>Ag</u>	<u>W</u>	<u>F</u>
			Parts per million						
Control	6	mean	54	7	11	1.3	0.5	9	795
		std.dev.	8	9	2	0.5	0.3	9	275
QPP	22	mean	14	20	7	218	0.6	20	370
		std.dev.	8	15	3	275	0.3	17	139

APPENDIX V

Normative Compositions and Ratios for QPP

Normative compositions were calculated in the order: ferromagnesian and alkali minerals, then corundum and quartz.

<u>Sample Number</u>	<u>Quartz</u>	<u>Corundum</u>	<u>Quartz : Albite : Orthoclase</u>		
			Per cent		
01	61.4	6.8	65.8	: 2.1	: 32.1
02	51.7	6.5	55.5	: 3.2	: 41.3
03	52.2	9.9	60.3	: 2.3	: 37.4
04	70.3	7.8	76.1	: 1.1	: 22.9
06	60.4	7.7	65.8	: 2.2	: 32.1
07	76.1	5.9	81.7	: 2.1	: 16.2
09	75.4	4.6	79.9	: 2.1	: 18.0
10	67.7	6.9	73.6	: -	: 26.4
11	66.3	8.7	73.4	: 1.1	: 25.5
13	63.0	3.8	65.2	: 3.1	: 31.7
14	67.0	7.1	71.8	: -	: 28.2
15	55.2	5.4	59.2	: 2.1	: 38.7
16	57.6	5.7	62.3	: 3.2	: 34.5
18	69.5	2.6	71.2	: 3.0	: 25.8
21	54.7	5.9	59.5	: 2.2	: 38.3
22	63.8	8.8	70.3	: -	: 29.7
23	63.3	6.6	66.9	: 2.1	: 31.0
25	64.4	7.9	70.3	: 2.2	: 27.5
29	56.8	9.0	66.1	: -	: 33.9
33	67.4	4.7	71.0	: -	: 29.0
average	63.2	6.6	68.3	: 1.7	: 30.0